INFLUENCE OF VOLUME FRACTION OF DUST PARTICLES ON DUSTY FLUID FLOW THROUGH POROUS RECTANGULAR CHANNEL

K R MADHURA[1], D S SWETHA[2]

[1] *Post Graduate Department of Mathematics, The National College, Jayanagar, Bangalore, Trans - Disciplinary Research Centre, National Degree College, Basavanagudi and The Florida International University, USA*

[2] *Department of Mathematics, PES University, Bangalore, India*

Research Scholar : East West Institute of Technology, VTU, Karnataka, India.

Abstract :*This article provides a novel solutions to unsteady flow of dusty fluid passing through porous rectangular channel with the consideration of volume fraction of dust particles. Effects of magnetic parameter, porous parameter and volume fraction of dust particles on both fluid and dust velocity profiles under different boundary conditions are analysed. Results are exhibited both analytically and numerically after solving the non-dimensional governing equations using Laplace transform, Fourier transform and Crank-Nicolson methods. Mathlab software is used to obtain numerical computation. The effects of pertinent parameters are also exhibited in tabular and graphical forms. For the interest of physical and engineering field, skin friction at the boundaries are calculated.*

Keywords: *Dusty fluid, rectangular channel, volume fraction of dust particles, porous medium.*

AMS Subject Classification (2000): 76T10, 76T15.

1. Introduction

Over the course of more than decades, interest in problems of systems with more than one phase has developed rapidly which leads to the study of the flow of a dusty fluids and also gains more attention of scientists due to its enormous applications in industries, engineering sciences, scientific fields such as oil and gas recovery, water flooding, enhanced oil recovery, X-ray tomography, terahertz tomography, geological materials, liquid foams, polymer fluids, slurries, nuclear engineering, biology, meteorology and physics etc. In addition, it is desirable to analyse an important class of multi-phase flow referred as porous medium which is crucial to many technological applications like filtering water, squeezing a wet sponge, brewing coffee etc.

Volume fraction of dust particles have been the topics of extensive research due to their applications in many branches includes miscible and immiscible fluid animation, volume of fluid technique, medical imaging applications, bubble columns, interphase interactions etc. Inspite of this, volume fraction plays a vital role in the motion of the fluids having high fluid density like bromine, liquid metal, mercury etc. It is therefore of interest to investigate the results of flow computations, if volume fraction of the dust particles are considered and also it is imperative to establish the conditions at which this parameter should be included in a flow analysis. For instance, Saffman [1] has studied the laminar flow of a dusty fluid by neglecting the volume fraction of the dust particles. Later, for the same flow, Gupta and Gupta [2] have established the results by taking the volume fraction of dust particles into consideration and justified the importance of volume fraction of dust particles on motion of fluids. Apart from that, Rudinger [3] has shown that the error introduced in a flow analysis of gas particles mixtures by neglecting the volume fraction of dust particles. Sagdeev et al. [4] and Miura et al. [5] have obtained an analytical solutions of a planar dusty gas flow with constant velocities of the

Nomenclature:

$\overrightarrow{u}$ - velocity of the fluid phase	$\overrightarrow{v}$ - velocity of the dust phase
k - $6\pi a_1\mu$ - stokes resistance coefficient	t - time
a_1 -spherical radius of the dust particle	m - mass of the dust particle
N_0 - number density of the dust particles	G_x - resultant body force on the fluid
ϕ - volume fraction of the dust particles	ρ - density of the fluid
σ - electrical conductivity	μ - the coefficient of viscosity of fluid particles
p - pressure of the fluid	β_0 - intensity of the imposed transverse magnetic field
η - permeability of the porous medium	ν - kinematic viscosity
M - magnetic parameter	δ - spin gradient viscosity
S_1 - thermal dispersion	

shock and the piston moving behind it. As they neglected the volume fraction of the solid particles, the dust virtually had a mass fraction but no volume fraction and hence their results reflect the influence of the additional inertial of the dust upon the shock.

Multiphase flows are common in many sectors and the attainment of the volume fraction of each element is challenging for the engineering process, henceforth, determining them is very influential. Consequently, Robson Ramos et al. [6] have presented a methodology for determination of volume fractions in annular three-phase flow systems such as oil-water-gas based on the use of nuclear techniques and artificial intelligence. N.Aquelet et al. [7] have described volume fraction initialisation algorithm which improves the flexibility and efficiency of multi-material ALE codes. Accordingly, numerical fluid leakage through the edifice involving an erroneous solution of the coupling algorithm can be avoided due to immoral volume fraction initialisation. Volume fraction based approach is proposed by Kai Bao et al. [8] to simulate miscible and immiscible flows simultaneously and they have exhibited that techniques involved in simulation shows good controllabilty and different mixing effects can be obtained by adjusting the dynamics viscosities and diffusion coefficients. Nayfeh [9] has formulated the equations of motion of the fluid particles taking the volume fraction of the dust particles into account. Investigation by Sana Ahsan [10] on volume fraction influence of dusty fluid flow between parallel plates and results revealed that fluid velocity and particle velocity are provoked by magnetic field for different values of volume fraction and non Newtonian factor. By using Saffman's model and oldroyd model, Debasish Dey [11] has found the solutions for unsteady dusty electrically conducting oldroyd fluid flow in presence of volume fraction and energy dissipation. Rakesh kumar [12] has presented a study on particulate couette flow with volume fraction of dust particles and numerical computations are obtained to spectacle the effects of innumerable constraints involved. MHD effects on convective flow of dusty viscous fluid with volume fraction of dust particles was studied by Ibrahim Saidu et al. [13] and they have predicted that velocity of liquid and dust particles decreases with the increase in the porous parameter. R.K.Gupta and S.N.Gupta [14] have made an exhaustive theoritical study on unsteady flow of a dusty fluid through ducts and shows the prominence of volume fraction assortment for the validity of Saffman model.

Tremendous applications attracted the investigators to investigate on fluid flow through different channels, predominantly in the field of industrial and chemical engineering such as particles in emulsion paints, reinforcing particles in polymers melts and rock crystals in molten lava etc. Anil Tripathi et al. [15] have investigated the effect of magnetic field on the flow of dusty visco-elastic second order oldroyd fluid through a long rectangular channel by captivating very small Reynolds number. Using the open rectangular geometry, K.R.Madhura et al. [16] have employed Laplace and finite Fourier sine transform methods to obtain solutions for flow of an unsteady dusty fluid through porous media. Using the same rectangular geometry, Singh [17] has analysed dusty fluid flow by considering different time dependent pressure gradients. Ruchi Chaturvedi [18] has adopted fast converging numerical implicit scheme to solve dimensionless governing equations for a dusty fluid flow passing through porous medium. B.C.Prasannakumara et al. [19] have discussed the variation of velocity and temperature fields with respect to melting process of the stretching sheet in presence of thermal radiation and non-uniform heat source/sink. To investigate effects of the elasticity on the flow resistance, Hai Long Liu et al. [20] presented flow simulations of viscoelastic fluids in the unidirectional fibrous porous media. Along with the above cited papers, several authors like Singh and Ram [21], Prasad and Ramacharyulu [22], Nag [23], B.J.Gireesha [24], Ali.J.Chamka [25], C.L.Varshney [26], P.T.Manjunatha [27], Akhilesh K. Sahu [28] have studied different flow patterns through channels of various cross-sections by considering different time dependent pressure gradients.

Aforementioned studies reveals the vital role of geometries in the fluid flow characteristics and in this study, predominantly rectangular shape is considered due to its special possessions.

- Analysis by Michael Schriber [29] illustrated that the models involving rectangular geometry favours in optimizing conduit shapes for drug delivery or for chemical reaction vessels.
- As the system having low frequency is proportional to its internal volume and also the rectangular geometry offers good internal volume results into the greater the internal volume, the greater the low frequency output approximation.

Keeping all these specifics in mind and to the best of author's knowledge, research on unsteady dusty fluid flow by taking volume fraction of dust particles into consideration through two-dimensional geometry, particularly rectangular channel has consequences in various fields and till date little attention has been shown. Therefore, the core dispassionate of the present study is to establish detailed analysis on two-dimensional numerical and analytical approach on dusty fluid flow with the consideration of volume fraction of dust particles and to interpret the effects of pertinent parameters on velocity profiles. The authors have hope that the results obtained in the present study not only provide useful information for applications, it also serves as a complement to the previous studies.

2. Mathematical Analysis

Consider an unsteady, laminar flow of a incompressible, viscous fluid through porous medium of a rectangular channel with volume fraction of the dust particles taken into account and the governing equations of motion are written in the following form :

For fluid phase:

$$\rho(1-\phi)\frac{\partial \vec{u}}{\partial t} = (1-\phi)\left[-\frac{\partial p}{\partial z} + \mu\left(\frac{\partial^2 \vec{u}}{\partial x^2} + \frac{\partial^2 \vec{u}}{\partial y^2}\right)\right] + kN_0(\vec{v}-\vec{u}) - \sigma\beta_0^2\vec{u} + G_x - \frac{\mu}{\eta}\vec{u} \tag{1}$$

For dust phase:

$$N_0 m\frac{\partial \vec{v}}{\partial t} = \phi\left[-\frac{\partial p}{\partial z} + \mu\left(\frac{\partial^2 \vec{u}}{\partial x^2} + \frac{\partial^2 \vec{u}}{\partial y^2}\right)\right] + kN_0(\vec{u}-\vec{v}) \tag{2}$$

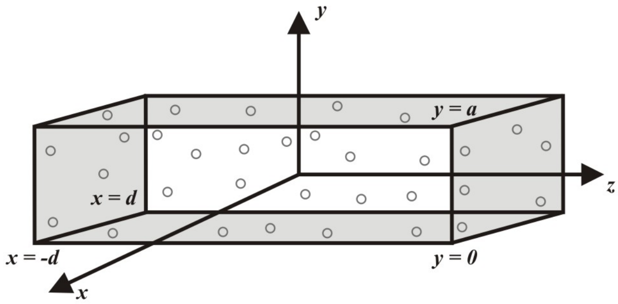

Fig. 1 : Schematic diagram of the dusty fluid flow through porous rectangular channel

The analysis is based on the following assumptions :

- The dust particles are spherical in shape, equal in size and uniformly distributed in the flow region.
- The volume occupied by the particles per unit volume of the mixture (i.e. volume fraction of dust particles) have been taken into consideration.
- Both the fluid and the dust particle clouds are static at the beginning.
- Using a rectangular cartesian coordinate system (x, y, z) such that z - axis is along the axis of the channel and the walls of the channel are bounded between $x = -d, x = d, y = 0, y = a$.

Taken into consideration of these assumptions for the flow through rectangular channel, the velocity components of fluid and dust particles are respectively given by :

$$\vec{u} = u_z\,\vec{z}, \qquad \vec{v} = v_z\,\vec{z} \tag{3}$$

i.e., $u_x = u_y = 0$ and $v_x = v_y = 0$ where (u_x, u_y, u_z) and (v_x, v_y, v_z) denote the velocity components of fluid and dust phases respectively.

Equations(1), (2) are to be solved by subjecting to the initial and boundary conditions;

Initial condition : at t = 0, $u_z = v_z = 0$

Boundary condition: for $t > 0$,

$$u_z = v_z = 0 \text{ at } x = \pm d$$
$$u_z = v_z = g(t) \text{ at } y = a$$
$$\frac{\partial u_z}{\partial y} = \frac{\partial v_z}{\partial y} = 0 \text{ at } y = 0 \tag{4}$$

Using the following non-dimensional quantities, equations (1), (2) and boundary condition becomes as follows;
$x = ax^*$, $y = ay^*$, $z = az^*$, $pa^2 = \rho\nu^2 p^*$, $t\nu = a^2 t^*$, $au_z = \nu u_z^*$, $av_z = \nu v_z^*$;

$$\frac{\partial u_z}{\partial t} = -\frac{\partial p}{\partial z} + \left(\frac{\partial^2 u_z}{\partial x^2} + \frac{\partial^2 u_z}{\partial y^2}\right) + \epsilon_1 (v_z - u_z)$$
$$- Mu_z + S_1 - \frac{a^2}{\eta(1-\phi)} u_z \tag{5}$$

$$\frac{\partial v_z}{\partial t} = \phi' \left[-\frac{\partial p}{\partial z} + \left(\frac{\partial^2 u_z}{\partial x^2} + \frac{\partial^2 u_z}{\partial y^2}\right)\right] + \delta (u_z - v_z) \tag{6}$$

where
$M = \frac{\sigma\beta_0^2 a^2}{\mu(1-\phi)}$, $S_1 = \frac{G_x a^3}{\rho\nu^2 (1-\phi)}$, $f = \frac{mN_0}{\rho}$, $\phi' = \frac{\phi}{f}$,
$\delta = \frac{ka^2}{m\nu}$, $\epsilon = \frac{\delta}{(1-\phi)}$, $\epsilon_1 = f\epsilon$.
The corresponding boundary conditions reduces to:

$$u_z = v_z = 0 \text{ at } x = \pm \frac{d}{a}$$
$$u_z = v_z = g(t) \text{ at } y = 1$$
$$\frac{\partial u_z}{\partial y} = \frac{\partial v_z}{\partial y} = 0 \text{ at } y = 0 \tag{7}$$

Let $-\frac{\partial p}{\partial z} = u_0$, where u_0 is a constant.
Expound the Laplace transform of u and v as,

$\overline{u} = \int_0^\infty e^{-st} u_z \, dt$, $\overline{v} = \int_0^\infty e^{-st} v_z \, dt$
Applying the Laplace transform to equations (5), (6)

$$s\,\overline{u} = \frac{u_0}{s} + \left(\frac{\partial^2 \overline{u}}{\partial x^2} + \frac{\partial^2 \overline{u}}{\partial y^2}\right) + \epsilon_1 (\overline{v} - \overline{u})$$
$$- M\overline{u} + \frac{S_1}{s} - \frac{a^2}{\eta(1-\phi)} \overline{u} \tag{8}$$

$$s\,\overline{v} = \phi' \left[\frac{u_0}{s} + \left(\frac{\partial^2 \overline{u}}{\partial x^2} + \frac{\partial^2 \overline{u}}{\partial y^2}\right)\right] + \delta (\overline{u} - \overline{v}) \tag{9}$$

Boundary conditions becomes as follows:

$$\overline{u} = \overline{v} = 0 \text{ at } x = \pm \frac{d}{a}$$
$$\overline{u} = \overline{v} = G(s) \text{ at } y = 1$$
$$\frac{\partial \overline{u}}{\partial y} = \frac{\partial \overline{v}}{\partial y} = 0 \text{ at } y = 0 \tag{10}$$

where $G(s)$ is the Laplace transform of $g(t)$.
Rewriting the equations (8),(9) we get,

$$\left(s + M + \epsilon_1 + \frac{a^2}{\eta(1-\phi)}\right) \overline{u} = \left(\frac{\partial^2 \overline{u}}{\partial x^2} + \frac{\partial^2 \overline{u}}{\partial y^2}\right) + \epsilon_1 \overline{v}$$
$$+ \left(\frac{u_0}{s} + \frac{S_1}{s}\right) \tag{11}$$

$$\left(\frac{s+\delta}{\phi'}\right) \overline{v} = \frac{u_0}{s} + \left(\frac{\partial^2 \overline{u}}{\partial x^2} + \frac{\partial^2 \overline{u}}{\partial y^2}\right) + \frac{\delta}{\phi'} \overline{u} \tag{12}$$

Applying finite Fourier transform to (11),(12) and then to (10)

$$\frac{\partial^2 \overline{u}_F}{\partial y^2} - \left(s + M + \epsilon_1 + \frac{a^2}{\eta(1-\phi)} + \frac{a^2 r^2 \pi^2}{d^2}\right) \overline{u}_F$$
$$+ \epsilon_1 \overline{v}_F = 0 \tag{13}$$

$$\frac{\partial^2 \overline{u}_F}{\partial y^2} + \left(\frac{\delta}{\phi'} - \frac{a^2 r^2 \pi^2}{d^2}\right) \overline{u}_F - \left(\frac{s+\delta}{\phi'}\right) \overline{v}_F = 0 \tag{14}$$

Boundary conditions reduces to as follows

$$\overline{u}_F = \overline{v}_F = 0 \text{ at } x = \pm \frac{d}{a}$$
$$\overline{u}_F = \overline{v}_F = G_F(s) \text{ at } y = 1$$
$$\frac{\partial \overline{u}_F}{\partial y} = \frac{\partial \overline{v}_F}{\partial y} = 0 \text{ at } y = 0 \tag{15}$$

where $G_F(s)$ is the finite Fourier sine transform of G(s) and

$$\overline{u}_F = \int_0^{d/a} \overline{u} \sin\left(\frac{r\pi x}{d/a}\right) dx, \quad \overline{v}_F = \int_0^{d/a} \overline{v} \sin\left(\frac{r\pi x}{d/a}\right) dx$$

Case-1 :
In this case, consider $g(t) = u_1$, where u_1 is a constant. Then the solutions of the equations (13) and (14) are given by

$$\overline{u}_F = \sum_{r=1}^{\infty} \frac{2u_1 d\,(1 - (-1)^r) \cosh(Ay)}{r\pi\nu s \cosh(A)} \tag{16}$$

$$\overline{v}_F = \sum_{r=1}^{\infty} \frac{2u_1 d\,(1 - (-1)^r) \cosh(Ay)}{r\pi\nu s \cosh(A)} \left(\frac{c_1 - A^2}{c_2}\right) \tag{17}$$

By applying inverse finite Fourier sine transform to the above equations, it takes the following form :

$$\overline{u} = \sum_{r=1}^{\infty} \frac{4au_1\,(1 - (-1)^r) \cosh(Ay)}{r\pi\nu s \cosh(A)} \sin\left(\frac{ar\pi x}{d}\right) \tag{18}$$

$$\overline{v} = \sum_{r=1}^{\infty} \frac{4au_1\,(1 - (-1)^r) \cosh(Ay)}{r\pi\nu s \cosh(A)} \left(\frac{c_1 - A^2}{c_2}\right)$$
$$\times \sin\left(\frac{ar\pi x}{d}\right) \tag{19}$$

Finally, the inverse Laplace transform of $\overline{u}$ and $\overline{v}$ are as follows :

$$u_z = \sum_{r=1}^{\infty} \frac{4au_1\left(1-(-1)^r\right)\cosh(\sqrt{c_{11}}\,y)}{r\pi\nu\cosh\left(\sqrt{c_{11}}\right)} \sin\left(\frac{ar\pi x}{d}\right) + \sum_{r=1}^{\infty}\sum_{n=0}^{\infty} \frac{4(2n+1)au_1d^2\left(1-(-1)^r\right) cos\left(\frac{(2n+1)\pi}{2}y\right)}{\nu r\,(-1)^n} \times \sin\left(\frac{ar\pi x}{d}\right)(C_1+D_1) \tag{20}$$

$$v_z = \sum_{r=1}^{\infty} \frac{4au_1\left(1-(-1)^r\right)\cosh(\sqrt{c_{11}}\,y)\,(c_{15}-c_{11})}{r\pi\nu c_2\cosh\left(\sqrt{c_{11}}\right)} \times \sin\left(\frac{ar\pi x}{d}\right) + 4au_1d^2\sin\left(\frac{ar\pi x}{d}\right)(C_2+D_2) \times \sum_{r=1}^{\infty}\sum_{n=0}^{\infty} \frac{(2n+1)\left(1-(-1)^r\right) cos\left(\frac{(2n+1)\pi}{2}y\right)}{\nu r c_2\,(-1)^n} \tag{21}$$

Shear stress (Skin friction): The explicit expression for shear stress on the wall at $x=\pm\frac{d}{a}$, $y=0$ respectively are given by:

$$D_{\pm\frac{d}{a},y} = \sum_{r=1}^{\infty} \frac{4a^2u_1\mu\,(-1)^r\left(1-(-1)^r\right)\cosh(\sqrt{c_{11}}\,y)}{d\nu\cosh\left(\sqrt{c_{11}}\right)} + \sum_{r=1}^{\infty}\sum_{n=0}^{\infty} \frac{4\pi(2n+1)a^2u_1d\mu\left(1-(-1)^r\right) cos\left(\frac{(2n+1)\pi}{2}y\right)}{\nu\,(-1)^{n-r}} \times (C_1+D_1) \tag{22}$$

$$D_{x,1} = \sum_{r=1}^{\infty} \frac{4a^2u_1\mu\left(1-(-1)^r\right)\cos\left(\frac{ar\pi x}{d}\right)}{d\nu} - \sum_{r=1}^{\infty}\frac{4au_1\mu}{\pi\nu} \times \frac{\left(1-(-1)^r\right)\sqrt{c_{11}}\tanh\left(\sqrt{c_{11}}\right)}{r}\sin\left(\frac{ar\pi x}{d}\right) + \sum_{r=1}^{\infty}\sum_{n=0}^{\infty} \frac{2(2n+1)^2au_1d^2\mu\pi\left(1-(-1)^r\right)}{\nu r}\sin\left(\frac{ar\pi x}{d}\right) \times (C_1+D_1) \tag{23}$$

Case-2 : In this case, let $g(t) = u_2\left(1+\alpha\cos(\beta t)\right)$, where u_2, α, β are constants.
Employing the same procedure as in case-1, one can obtain u_z and v_z as given below :

$$u_z = \sum_{r=1}^{\infty} \frac{4au_2\left(1-(-1)^r\right)\cosh(\sqrt{c_{11}}\,y)}{r\pi\nu\cosh\left(\sqrt{c_{11}}\right)} \sin\left(\frac{ar\pi x}{d}\right) + \sum_{r=1}^{\infty}\sum_{n=0}^{\infty} \frac{4(2n+1)au_2d^2\left(1-(-1)^r\right) cos\left(\frac{(2n+1)\pi}{2}y\right)}{\nu r\,(-1)^n} \times \sin\left(\frac{ar\pi x}{d}\right)(C_1+D_1) + \sum_{r=1}^{\infty}\sum_{n=0}^{\infty} \frac{4(2n+1)au_2d^2\alpha\left(1-(-1)^r\right) cos\left(\frac{(2n+1)\pi}{2}y\right)}{\nu r\,(-1)^n} \times \sin\left(\frac{ar\pi x}{d}\right)(C_3+D_3) + \sum_{r=1}^{\infty}\left(\frac{4au_2\alpha\left(1-(-1)^r\right)}{\nu r\pi\left(G^2+H^2\right)}\right)\sin\left(\frac{ar\pi x}{d}\right)\left[(EG+FH) \times \cos(\lambda_1 t) - (EH-FG)\sin(\lambda_1 t)\right] \tag{24}$$

$$v_z = \sum_{r=1}^{\infty} \frac{4au_2\left(1-(-1)^r\right)\cosh(\sqrt{c_{11}}\,y)\,(c_{15}-c_{11})}{r\pi\nu c_2\cosh\left(\sqrt{c_{11}}\right)} \times \sin\left(\frac{ar\pi x}{d}\right) + 4au_2d^2\sin\left(\frac{ar\pi x}{d}\right)(C_2+D_2) \times \sum_{r=1}^{\infty}\sum_{n=0}^{\infty} \frac{(2n+1)\left(1-(-1)^r\right) cos\left(\frac{(2n+1)\pi}{2}y\right)}{\nu r c_2\,(-1)^n} + \sum_{r=1}^{\infty}\sum_{n=0}^{\infty} \frac{4(2n+1)au_2d^2\alpha\left(1-(-1)^r\right) cos\left(\frac{(2n+1)\pi}{2}y\right)}{\nu r c_2\,(-1)^n} \times \sin\left(\frac{ar\pi x}{d}\right)(C_4+D_4) + \left(X_1\cos(\lambda_1 t) - X_2\sin(\lambda_1 t)\right) \times \sum_{r=1}^{\infty}\left(\frac{4au_2\alpha\left(1-(-1)^r\right)}{\nu r\pi c_2\left(G^2+H^2\right)}\right)\sin\left(\frac{ar\pi x}{d}\right) \tag{25}$$

Shear stress (Skin friction): The explicit expression for shear stress on the wall at $x=\pm\frac{d}{a}$, $y=0$, respectively are given by:

$$D_{\pm\frac{d}{a},y} = \sum_{r=1}^{\infty} \frac{4a^2u_2\mu\,(-1)^r)\left(1-(-1)^r\right)\cosh(\sqrt{c_{11}}\,y)}{d\nu\cosh\left(\sqrt{c_{11}}\right)} + \sum_{r=1}^{\infty}\sum_{n=0}^{\infty} \frac{4\pi(2n+1)a^2u_2d\mu\left(1-(-1)^r\right) cos\left(\frac{(2n+1)\pi}{2}y\right)}{\nu\,(-1)^{n-r}} \times (C_1+D_1) + \sum_{r=1}^{\infty}\sum_{n=0}^{\infty} \frac{4\pi(2n+1)a^2u_2d\alpha\mu\left(1-(-1)^r\right)}{\nu\,(-1)^{n-r}} \times (C_3+D_3)\,cos\left(\frac{(2n+1)\,\pi}{2}y\right) + \frac{4a^2u_2\alpha\mu}{\nu d\left(G^2+H^2\right)} \times \sum_{r=1}^{\infty}\frac{\left(1-(-1)^r\right)}{(-1)^r}\left[(EG+FH)\lambda_1 t - (EH-FG)\sin\lambda_1 t\right] \tag{26}$$

$$D_{x,1} = \sum_{r=1}^{\infty} \frac{4a^2 u_2 \mu \left(1-(-1)^r\right) \cos\left(\frac{ar\pi x}{d}\right)}{d\nu} - \sum_{r=1}^{\infty} \frac{4au_2\mu}{\pi\nu}$$
$$\times \frac{\left(1-(-1)^r\right)\sqrt{c_{11}} \tanh\left(\sqrt{c_{11}}\right)}{r} \sin\left(\frac{ar\pi x}{d}\right)$$
$$+ \sum_{r=1}^{\infty}\sum_{n=0}^{\infty} \frac{2(2n+1)^2 a u_2 d^2 \pi \mu \left(1-(-1)^r\right)}{\nu r} \sin\left(\frac{ar\pi x}{d}\right)$$
$$\times \left(C_1 + D_1\right) + \sum_{r=1}^{\infty} \frac{4a^2 u_2 \alpha \mu \left(1-(-1)^r\right) \cos\left(\frac{ar\pi x}{d}\right)}{d\nu\left(G^2+H^2\right)}$$
$$\times \left[\left(G^2+H^2\right)\cos\left(\lambda_1 t\right)\right] + \frac{2au_2 d^2 \alpha\pi\mu}{\nu}$$
$$\times \sum_{r=1}^{\infty}\sum_{n=0}^{\infty} \frac{(2n+1)^2\left(1-(-1)^r\right)}{r} \sin\left(\frac{ar\pi x}{d}\right)\left(C_3+D_3\right)$$
$$- \frac{4au_2\alpha\mu\left(1-(-1)^r\right)}{\nu r\pi\left(G^2+H^2\right)} \sin\left(\frac{ar\pi x}{d}\right)\left[\left(\alpha_2\cosh(\alpha_2)\sinh(\alpha_2)\right.\right.$$
$$-\beta_2\cos(\beta_2)\sin(\beta_2)\right)\cos\left(\lambda_1 t\right) + \left(\beta_2\cosh(\alpha_2)\sinh(\alpha_2)\right.$$
$$\left.\left.+\alpha_2\sin(\beta_2)\cos(\beta_2)\right)\sin\left(\lambda_1 t\right)\right] \quad (27)$$

3. Numerical Solutions

In the present situation, scientists are more fascinated towards numerical methods than analytical methods, as it reduces the difficulties of time consumption and solving techniques. Therefore, here the mathematical software Mathlab has been used to obtain numerical solutions for the same prescribed flow and Crank Nicolson technique is used to solve the partial differential equations (2.5) and (2.6) and is given by :

$$\left(\frac{1}{\triangle t} + \frac{1}{(\triangle x)^2} + \frac{1}{(\triangle y)^2}\right) u_{i,j}^{n+1} - \frac{1}{2(\triangle x)^2}$$
$$\left(u_{i+1,j}^{n+1} + u_{i-1,j}^{n+1}\right) - \frac{1}{2(\triangle y)^2}\left(u_{i,j+1}^{n+1} + u_{i,j-1}^{n+1}\right)$$
$$= \left(\frac{1}{\triangle t} - \frac{1}{(\triangle x)^2} - \frac{1}{(\triangle y)^2} - \epsilon_1 - M\right) u_{i,j}^{n}$$
$$+ \frac{1}{2(\triangle x)^2}\left(u_{i+1,j}^{n} + u_{i-1,j}^{n}\right) + \frac{1}{2(\triangle y)^2}\left(u_{i,j+1}^{n}\right.$$
$$\left.+u_{i,j-1}^{n}\right) + \epsilon_1 v_{i,j}^{n} + \left(u_{00} + S_1\right) \quad (28)$$

$$\frac{1}{\triangle t} v_{i,j}^{n+1} - \frac{\phi'}{2(\triangle x)^2}\left(u_{i+1,j}^{n+1} + u_{i-1,j}^{n+1}\right) - \frac{\phi'}{2(\triangle y)^2}$$
$$\left(u_{i,j+1}^{n+1} + u_{i,j-1}^{n+1}\right) + \left(\frac{\phi'}{(\triangle x)^2} + \frac{\phi'}{(\triangle y)^2}\right) u_{i,j}^{n+1}$$
$$= \left(-\frac{\phi'}{(\triangle x)^2} - \frac{\phi'}{(\triangle y)^2} + \delta\right) u_{i,j}^{n} + \left(\frac{1}{\triangle t} - \delta\right) v_{i,j}^{n}$$
$$+ \frac{\phi'}{2(\triangle x)^2}\left(u_{i+1,j}^{n} + u_{i-1,j}^{n}\right) + \frac{\phi'}{2(\triangle y)^2}\left(u_{i,j+1}^{n}\right.$$
$$\left.+u_{i,j-1}^{n}\right) - \phi' u_{00} \quad (29)$$

Case-1 :

The initial and boundary conditions are given by :

$$\text{For} \quad t = 0, \quad u_{i,j}^0 = v_{i,j}^0 = 0$$
$$\text{For} \quad t > 0, \quad u_{-1,j}^n = v_{-1,j}^n = 0 \ \text{at} \ x = -1$$
$$u_{n_1,j}^n = v_{n_1,j}^n = 0 \ \text{at} \ x = 1$$
$$u_{i,0}^n = v_{i,0}^n = \frac{au_1}{\nu} \ \text{at} \ y = 0$$
$$\frac{u_{i,0} - u_{i,n}}{\triangle y} = \frac{v_{i,0} - v_{i,n}}{\triangle y} = 0 \ \text{at} \ y = 1$$

Case-2 :

The initial and boundary conditions are represented as follows :

$$\text{For} \quad t = 0, \quad u_{i,j}^0 = v_{i,j}^0 = 0$$
$$\text{For} \quad t > 0, \quad u_{-1,j}^n = v_{-1,j}^n = 0 \ \text{at} \ x = -1$$
$$u_{n_1,j}^n = v_{n_1,j}^n = 0 \ \text{at} \ x = 1$$
$$u_{i,0}^n = v_{i,0}^n = \frac{au_2}{\nu}\left(1 + \alpha\cos\left(\lambda_1 t\right)\right) \ \text{at} \ y = 0$$
$$\frac{u_{i,0} - u_{i,n}}{\triangle y} = \frac{v_{i,0} - v_{i,n}}{\triangle y} = 0 \ \text{at} \ y = 1$$

Here, rectangular computational domain is used with grid point distribution at unequal spacing such that i refers to x, j refers to y with step size of $\triangle x = 1$, $\triangle y = 0.25$ and n refers to time t with its mesh $\triangle t = 0.05$ was selected. Throughout our analysis for numerical and analytical results, we have employed $\triangle x = 1$, $\triangle y = 0.25$, $a = 0.25$, $d = 1$, $u_1 = 0.2$, $\kappa = 0.3$, $N_0 = 0.1$, $M = 5$, $m = 0.2$, $\nu = 0.2$, $\eta = 0.2$, $\rho = 0.1$,$u_2 = 0.1$, $t = 0.2$ and to judge the accuracy of the convergence and stability of numerical techniques, the outcomes have computed with smaller values of $\triangle x$, $\triangle y$ i.e., $\triangle x = 1,\ 0.5,\ 0.25$ etc. and $\triangle y = 0.25,\ 0.125,\ 0.0625$ etc. The computations are iterated until to meet the convergence criteria at the streamwise position. The tables [1-12] reveals the numerical and analytical solutions of fluid and dust velocities for different values of volume fraction, magnetic parameter, porosity and noticed that there is a close agreement with these approaches and thus ensures the accuracy of the methods used.

International Journal of Mathematics Trends and Technology (IJMTT) - Volume 50 Number 5 October 2017

4. Results and discussions

The impact of volume fraction of dust particles on dusty fluid flow through rectangular channel are investigated in the presence of porous medium. The governing partial differential equations (5) and (6) are solved analytically using Laplace transform, Fourier transform and numerically using Crank-Nicolson methods. Variation of fluid and dust velocities for different values of volume fraction, magnetic parameter, porous parameter are shown in graphs [2-13] and exhibited the values through tables [1-12]. It is worth mentioning that the results obtained from both the methods are well in agreement. It is evident from the graphs that,

- The flow is parabolic in nature.
- The flow of fluid particles is parallel to that of dust.
- The fluid velocity is higher than the dust particles velocity since dust particles restrict the flow.

The following observations are obtained for the two cases i.e. $g(t) = u_1$ and $g(t) = u_2\left(1 + \alpha\cos\left(\beta t\right)\right)$, where u_1, u_2, α, β are constants.

a. Impact of volume fraction on fluid and dust velocity profiles

Graphs [2-5] and tables [1-4] depicts the velocity profiles of fluid and dust phases for disperate values of volume fraction of dust particles. In order to maintain Saffman's model, the range of volume fraction is choosen small. It is noticed that an increase in the volume fraction of dust particles, increases the velocity profiles for both fluid and dust phases. This behaviour is observed as the volume occupied by the dust particles per unit volume of the fluid is higher than the dust concentration i.e. fluid particles move faster than dust particles.

y	For $\phi = 0.04$											
	For $x = 1$				For $x = 2$				For $x = 3$			
	$u_e.$	u_n	v_e	v_n	u_e	u_n	v_e	v_n	u_e	u_n	v_e	v_n
0.25	0.0974	0.0976	0.0487	0.0488	0.1378	0.1379	0.0689	0.0690	0.0974	0.0976	0.0487	0.0488
0.50	0.1456	0.1458	0.0728	0.0729	0.2059	0.2060	0.1030	0.1032	0.1456	0.1458	0.0728	0.0729
0.75	0.2501	0.2502	0.1251	0.1252	0.3537	0.3539	0.1768	0.1769	0.2501	0.2502	0.1251	0.1252

Table 1. Comparison of exact and numerical solutions for fluid and dust velocity profiles for $\phi = 0.04$ (case-1)

y	For $\phi = 0.06$											
	For $x = 1$				For $x = 2$				For $x = 3$			
	$u_e.$	u_n	v_e	v_n	u_e	u_n	v_e	v_n	u_e	u_n	v_e	v_n
0.25	0.0993	0.0995	0.0497	0.0499	0.1405	0.1406	0.0702	0.0704	0.0993	0.0995	0.0497	0.0499
0.50	0.1470	0.1472	0.0735	0.0737	0.2079	0.2080	0.1040	0.1042	0.1470	0.1472	0.0735	0.0737
0.75	0.2511	0.2512	0.1255	0.1257	0.3551	0.3552	0.1775	0.1776	0.2511	0.2512	0.1255	0.1257

Table 2. Comparison of exact and numerical solutions for fluid and dust velocity profiles for $\phi = 0.06$ (case-1)

y	For $\phi = 0.04$											
	For $x = 1$				For $x = 2$				For $x = 3$			
	$u_e.$	u_n	v_e	v_n	u_e	u_n	v_e	v_n	u_e	u_n	v_e	v_n
0.25	0.1023	0.1025	0.0998	0.0998	0.1446	0.1447	0.1412	0.1412	0.1023	0.1025	0.0998	0.0998
0.50	0.1529	0.1530	0.1493	0.1492	0.2162	0.2164	0.2111	0.2110	0.1529	0.1530	0.1493	0.1492
0.75	0.2626	0.2628	0.2564	0.2566	0.3714	0.3718	0.3625	0.3627	0.2626	0.2628	0.2564	0.2566

Table 3. Comparison of exact and numerical solutions for fluid and dust velocity profiles for $\phi = 0.04$ (case-2)

y	For $\phi = 0.06$											
	For $x = 1$				For $x = 2$				For $x = 3$			
	u_e.	u_n	v_e	v_n	u_e	u_n	v_e	v_n	u_e	u_n	v_e	v_n
0.25	0.1043	0.1045	0.1018	0.1019	0.1475	0.1476	0.1440	0.1444	0.1043	0.1045	0.1018	0.1019
0.50	0.1544	0.1546	0.1507	0.1508	0.2183	0.2184	0.2131	0.2132	0.1544	0.1546	0.1507	0.1508
0.75	0.2636	0.2638	0.2574	0.2576	0.3728	0.3729	0.3640	0.3641	0.2636	0.2638	0.2574	0.2576

Table 4. Comparison of exact and numerical solutions for fluid and dust velocity profiles for $\phi = 0.06$ (case-2)

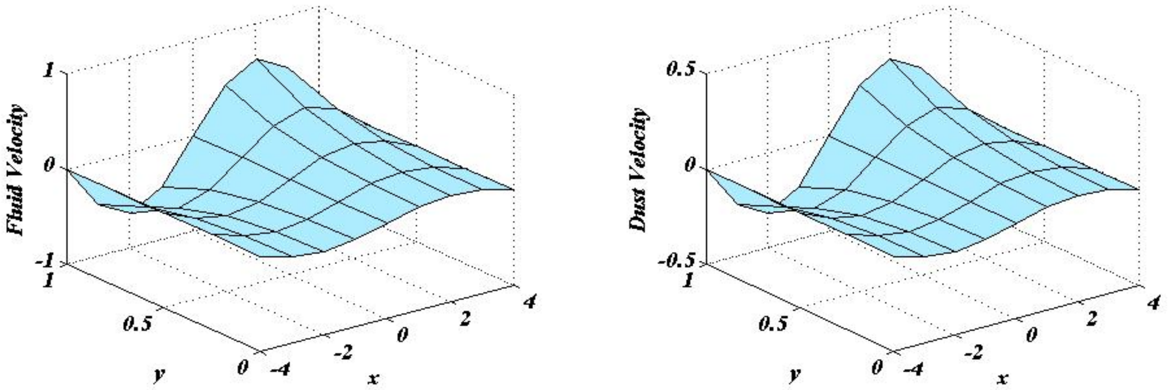

Fig. 2 : Variation of fluid and dust velocities when $\phi = 0.04\,(\text{case} - 1)$

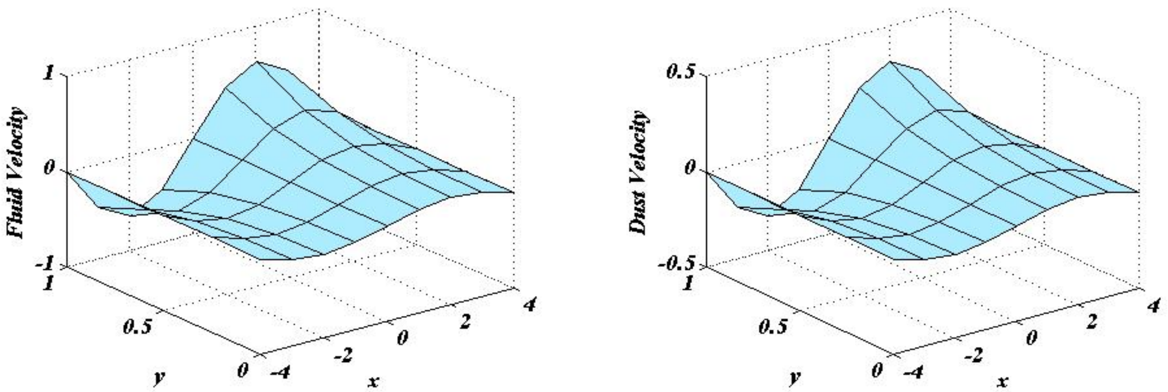

Fig. 3 : Variation of fluid and dust velocities when $\phi = 0.06\,(\text{case} - 1)$

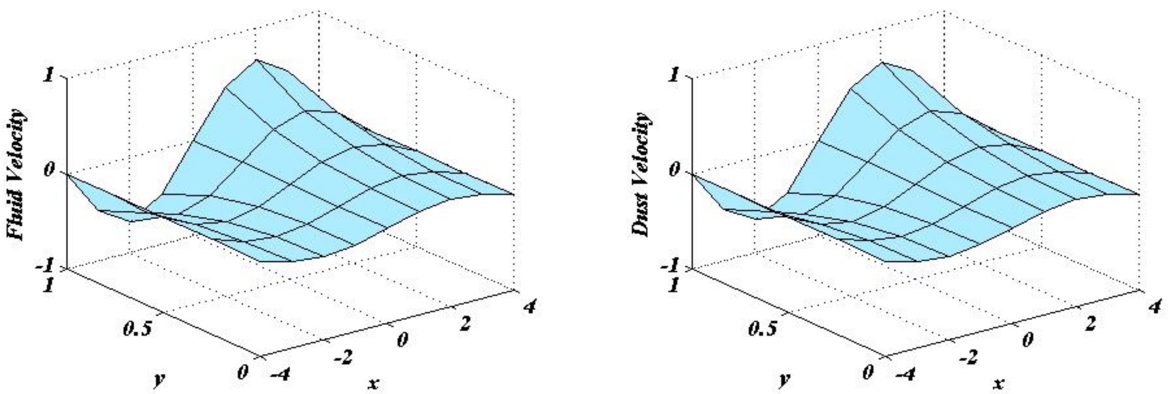

Fig. 4 : Variation of fluid and dust velocities when $\phi = 0.04\,(\text{case} - 2)$

International Journal of Mathematics Trends and Technology (IJMTT) - Volume 50 Number 5 October 2017

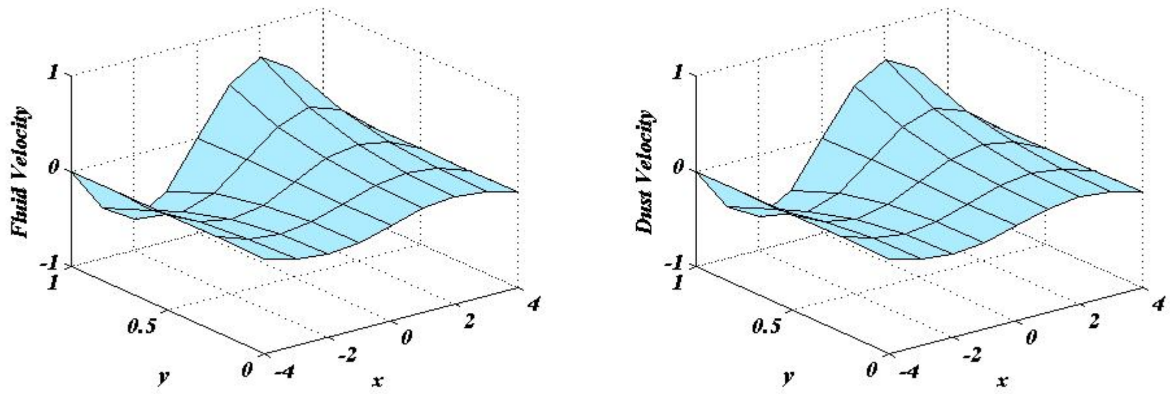

Fig. 5 : Variation of fluid and dust velocities when $\phi = 0.06\,(\text{case} - 2)$

b. Impact of magnetic parameter on fluid and dust velocity profiles

Graphs [6-9] and tables [5-8] shows the influence of magnetic parameter on velocity profiles and reveals that an increase in the magnetic parameter results in depreciation of velocity phases of fluid and dust. Physically, it is justified due to the fact that an infliction of magnetic field sets a drag-force called Lorentz force, which results in retarding effect on velocity field i.e. an increase in the magnetic field parameter produces opposite force to flow called the Lorentz force, which has a tendency to slow down the flow and hence fluid and dust velocity phases diminishes. This force also helps to enhance the thermal and concentration boundary layers.

y	For $M = 5$											
	For $x = 1$				For $x = 2$				For $x = 3$			
	$u_e.$	u_n	v_e	v_n	u_e	u_n	v_e	v_n	u_e	u_n	v_e	v_n
0.25	0.0974	0.0976	0.0487	0.0488	0.1378	0.1379	0.0689	0.0690	0.0974	0.0976	0.0487	0.0488
0.50	0.1456	0.1458	0.0728	0.0729	0.2059	0.2060	0.1030	0.1032	0.1456	0.1458	0.0728	0.0729
0.75	0.2501	0.2502	0.1251	0.1252	0.3537	0.3539	0.1768	0.1769	0.2501	0.2502	0.1251	0.1252

Table 5. Comparison of exact and numerical solutions for fluid and dust velocity profiles for $M = 5$ (case-1)

y	For $M = 10$											
	For $x = 1$				For $x = 2$				For $x = 3$			
	$u_e.$	u_n	v_e	v_n	u_e	u_n	v_e	v_n	u_e	u_n	v_e	v_n
0.25	0.0480	0.0481	0.0240	0.0241	0.0679	0.0678	0.0340	0.0341	0.0480	0.0481	0.0240	0.0241
0.50	0.0907	0.0907	0.0453	0.0455	0.1282	0.1283	0.0641	0.0643	0.0907	0.0907	0.0453	0.0455
0.75	0.1993	0.1994	0.0996	0.0997	0.2818	0.2820	0.1409	0.1409	0.1993	0.1994	0.0996	0.0997

Table 6. Comparison of exact and numerical solutions for fluid and dust velocity profiles for $M = 10$ (case-1)

y	For $M = 5$											
	For $x = 1$				For $x = 2$				For $x = 3$			
	$u_e.$	u_n	v_e	v_n	u_e	u_n	v_e	v_n	u_e	u_n	v_e	v_n
0.25	0.1023	0.1025	0.0998	0.0998	0.1446	0.1447	0.1412	0.1412	0.1023	0.1025	0.0998	0.0998
0.50	0.1529	0.1530	0.1493	0.1492	0.2162	0.2164	0.2111	0.2110	0.1529	0.1530	0.1493	0.1492
0.75	0.2626	0.2628	0.2564	0.2566	0.3714	0.3718	0.3625	0.3627	0.2626	0.2628	0.2564	0.2566

Table 7. Comparison of exact and numerical solutions for fluid and dust velocity profiles for $M = 5$ (case-2)

y	For $M = 10$											
	For $x = 1$				For $x = 2$				For $x = 3$			
	$u_e.$	u_n	v_e	v_n	u_e	u_n	v_e	v_n	u_e	u_n	v_e	v_n
0.25	0.0504	0.0504	0.0492	0.0493	0.0713	0.0714	0.0696	0.0697	0.0504	0.0504	0.0492	0.0493
0.50	0.0952	0.0953	0.0930	0.0931	0.1347	0.1348	0.1315	0.1316	0.0952	0.0953	0.0930	0.0931
0.75	0.2092	0.2094	0.2043	0.2045	0.2959	0.2964	0.2889	0.2890	0.2092	0.2094	0.2043	0.2045

Table 8. Comparison of exact and numerical solutions for fluid and dust velocity profiles for $M = 10$ (case-2)

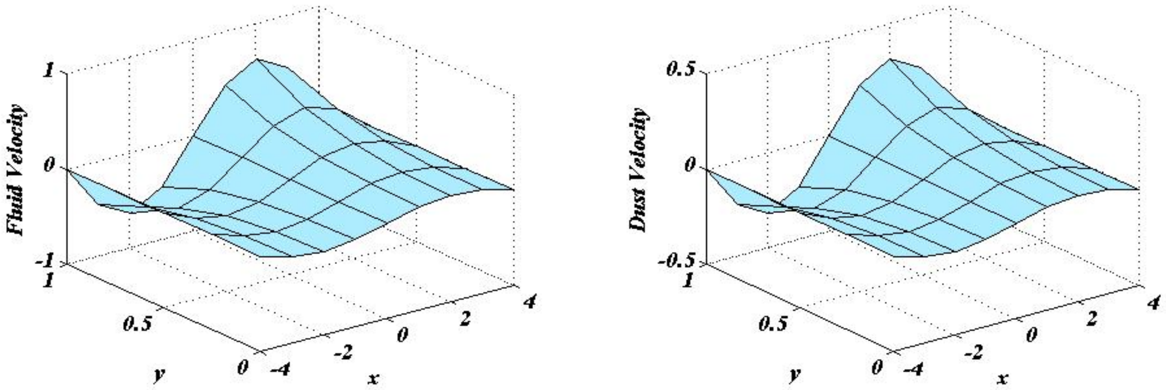

Fig. 6 : Variation of fluid and dust velocities when $M = 5\,(\text{case} - 1)$

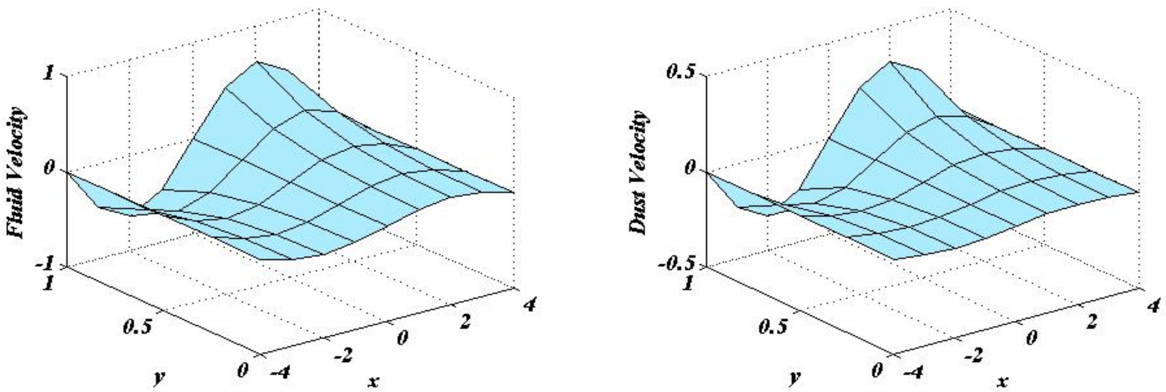

Fig. 7 : Variation of fluid and dust velocities when $M = 10\,(\text{case} - 1)$

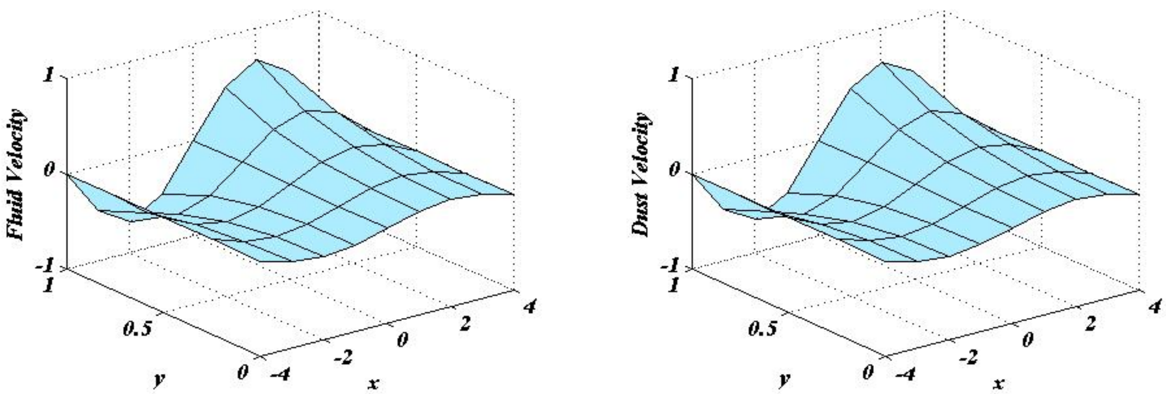

Fig. 8 : Variation of fluid and dust velocities when $M = 5\,(\text{case} - 2)$

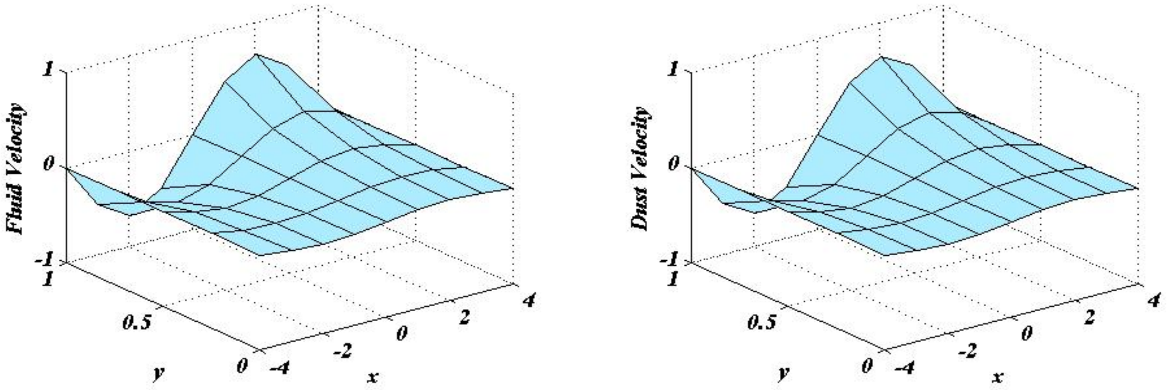

Fig. 9 : Variation of fluid and dust velocities when $M = 10\,(\text{case} - 2)$

c. Impact of permeability of porous medium on fluid and dust velocity profiles

Porosity is a fundamental microstructural parameter for most natural and man-made materials and significantly influences the physical properties of velocites, volume fraction etc. The porous parameter plays an important role on velocity profiles of both fluid and dust particles. The increase in porosity results in to decaying of drag like force called Lorentz force, this in turn a accelerating trend is observed in the motion of both fluid and dust phases and the same are demonstrated with the assist of graphs [10-13] and tables [9-12].

y	For $\eta = 0.2$											
	For $x = 1$				For $x = 2$				For $x = 3$			
	$u_e.$	u_n	v_e	v_n	u_e	u_n	v_e	v_n	u_e	u_n	v_e	v_n
0.25	0.0974	0.0976	0.0487	0.0488	0.1378	0.1379	0.0689	0.0690	0.0974	0.0976	0.0487	0.0488
0.50	0.1456	0.1458	0.0728	0.0729	0.2059	0.2060	0.1030	0.1032	0.1456	0.1458	0.0728	0.0729
0.75	0.2501	0.2502	0.1251	0.1252	0.3537	0.3539	0.1768	0.1769	0.2501	0.2502	0.1251	0.1252

Table 9. Comparison of exact and numerical solutions for fluid and dust velocity profiles for $\eta = 0.2$ (case-1)

y	For $\eta = 0.4$											
	For $x = 1$				For $x = 2$				For $x = 3$			
	$u_e.$	u_n	v_e	v_n	u_e	u_n	v_e	v_n	u_e	u_n	v_e	v_n
0.25	0.1001	0.1000	0.0501	0.0500	0.1416	0.1418	0.0708	0.0710	0.1001	0.1000	0.0501	0.0500
0.50	0.1484	0.1486	0.0742	0.0746	0.2099	0.2094	0.1049	0.1050	0.1484	0.1486	0.0742	0.0746
0.75	0.2524	0.2526	0.1262	0.1265	0.3569	0.3570	0.1785	0.1790	0.2524	0.2526	0.1262	0.1265

Table 10. Comparison of exact and numerical solutions for fluid and dust velocity profiles for $\eta = 0.4$ (case-1)

y	For $\eta = 0.2$											
	For $x = 1$				For $x = 2$				For $x = 3$			
	$u_e.$	u_n	v_e	v_n	u_e	u_n	v_e	v_n	u_e	u_n	v_e	v_n
0.25	0.1023	0.1025	0.0998	0.0998	0.1446	0.1447	0.1412	0.1412	0.1023	0.1025	0.0998	0.0998
0.50	0.1529	0.1530	0.1493	0.1492	0.2162	0.2164	0.2111	0.2110	0.1529	0.1530	0.1493	0.1492
0.75	0.2626	0.2628	0.2564	0.2566	0.3714	0.3718	0.3625	0.3627	0.2626	0.2628	0.2564	0.2566

Table 11. Comparison of exact and numerical solutions for fluid and dust velocity profiles for $\eta = 0.2$ (case-2)

y	For $\eta = 0.4$											
	For $x = 1$				For $x = 2$				For $x = 3$			
	$u_e.$	u_n	v_e	v_n	u_e	u_n	v_e	v_n	u_e	u_n	v_e	v_n
0.25	0.1052	0.1055	0.1027	0.1027	0.1487	0.1488	0.1452	0.1453	0.1052	0.1055	0.1027	0.1027
0.50	0.1558	0.1562	0.1521	0.1525	0.2204	0.2206	0.2151	0.2155	0.1558	0.1562	0.1521	0.1525
0.75	0.2650	0.2653	0.2587	0.2589	0.3748	0.3749	0.3658	0.3658	0.2650	0.2653	0.2587	0.2589

Table 12. Comparison of exact and numerical solutions for fluid and dust velocity profiles for $\eta = 0.4$ (case-2)

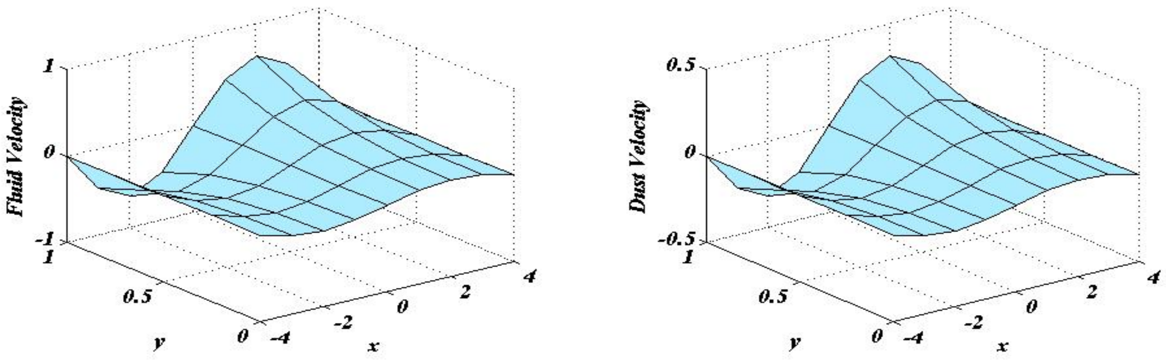

Fig. 10 : Variation of fluid and dust velocities when $\eta = 0.2\,(\text{case} - 1)$

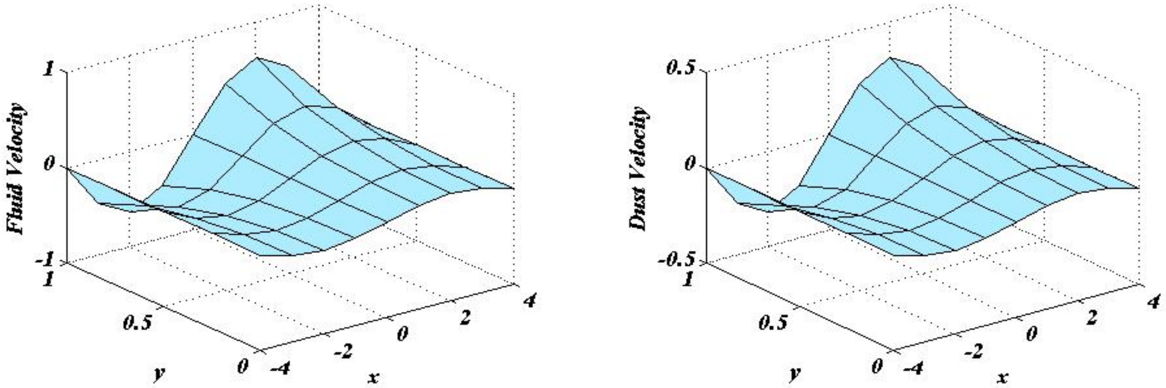

Fig. 11 : Variation of fluid and dust velocities when $\eta = 0.4\,(\text{case} - 1)$

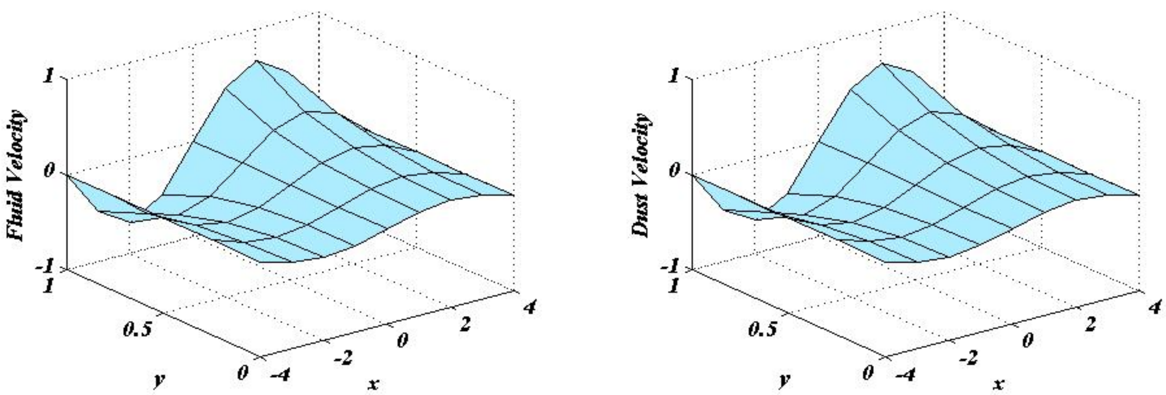

Fig. 12 : Variation of fluid and dust velocities when $\eta = 0.2\,(\text{case} - 2)$

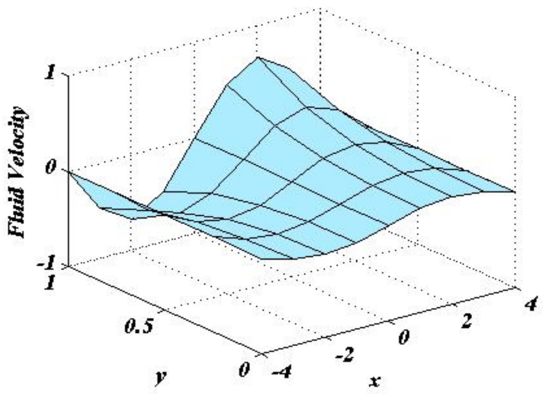

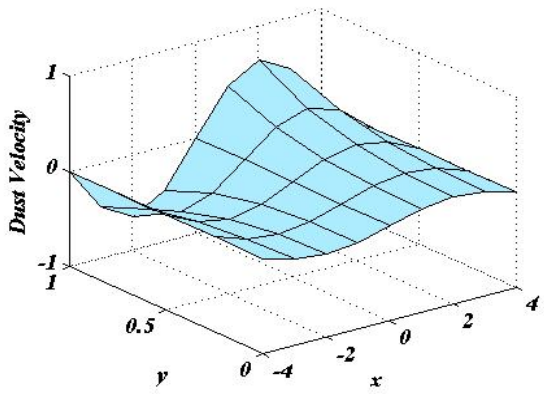

Fig. 13 : Variation of fluid and dust velocities when $\eta = 0.4\,(\text{case} - 2)$

5. Conclusions

A mathematical model has been developed to study the quantitative effects of different physical parameters on flow of dusty fluid passing through rectangular geometry embedded with porous material. Most important concluding remarks can be summarized as follows :

- Graphs [2-13] and tables [1-12] elucidate the variation of the volume fraction, magnetic parameter and porosity on velocity profiles for different boundary conditions as mentioned in case-1 and case-2.
- It is interesting to note that, the effects of above said parameters are same for both the cases i.e.
  i. Increase in volume fraction and porosity, increases the velocity profiles.
  ii. Increase in magnetic parameter, decreases the velocity profiles for both constant and pulsatile boundary conditions.

References

[1] P.G. Saffman, *On the stability of laminar flow of a dusty gas,* Journal of fluid mechanics, Vol. 13(1), pp. 120-128, 1962.

[2] P.K.Gupta, S.C.Gupta, *Flow of a dusty gas through a channel with arbitrary time varying pressure gradient*, J Appl Math Phys 27(1) (1976) 119-125.

[3] Rudinger G, *Some effects of finite particle volume on the dynamics of the gas-particle mixtures* , AIAA J 3(7) (1962) 1217-1222.

[4] Sagdeev, R.Z., M.A.Lepntovich,*Reviews of plasma physics*vol 4, Consultants Bureau, NEw York, (1966)p. 23.

[5] Miura, H.,Glass, I.I*Development of the flow induced by a piston impulsively in a dusty gas*, Proc. R. Soc. Lond. A 397, (1985) 295-309.

[6] Robson Ramos, Luis E.B.Brandao, Roberto Schirru, Cesar Marques Salgado, Claudio M.N.A.Pereira, Ademir Xavier da Silva, *Volume fraction calculation in multiphase system such as oil-water-gas using neutron*, International nuclear atlantic conference, (2007).

[7] N.Aquelet, C.Seddon, M.Souli, M.Moatamedi, *Initialisation of volume fraction in fluid/structure interaction problem*, IJCrash, 2(2005).

[8] Kai Bao, Xiaolong, Hui Zhang, Enhua Wu,*Volume fraction based miscible and immiscible fluid animation*, Computer animation and virtual worlds, (2010).

[9] Nayfeh A.H.,*Oscillating two-phase flow through a rigid pipe*, AIAA J , 4(10) (1966) 1868-1870.

[10] Sana Ahsan, *Effect of volume fraction on non newtonian flow of dusty fluid between two oscillating parallel plates,* International Journal of Emerging Technology and Innovative Engineering,1(7) (2015) 39-45.

[11] Debasish Deya, *Hydro-magnetic oscillatory dusty fluid with volume fraction and periodic pressure in a rotating channel* , International Journal for Research in Applied Science and Engineering Technology, 3(3) (2015) 869-877.

[12] Rakesh Kumar, *Particulate couette flow with volume fraction of dust particles*, Journal of Chemical, Biological and Physical Sciences 5(3) (2015) 2851-2862.

[13] I.Saidu, M.Y.Waziri, A.Roko, H.Musa, *MHD effects on convective flow of dusty viscous fluid with volume fraction of dust particles*, ARPN J. of Engg. and Applied Sciences, 5(10) (2010), 86-91.

[14] R.K.Gupta, S.N.Gupta, *Unsteady flow of a dusty fluid through ducts with volume fraction*, Proc. Indian natn. Sci. Acad, A 4 (1984) 350-364.

[15] Anil Tripathi, A.K.Sharma, K.K.Singh, *Effect of porous medium and magnetic field on the flow of dusty visco-elastic second order oldroyd fluid through a long rectangular channel*, International Journal of Mathematical Archive, 4(9) (2013), 243-247.

[16] K.R.Madhura, B.J.Gireesha, C.S.Bagewadi, *Exact solutions of unsteady dusty fluid flow through porous media in an open rectangular channel* Adv. Theor. Appl MEch, 2(1) (2009) 1-17.

[17] K.K.Singh, *Unsteady flow of a conducting dusty fluid through rectangular channel with time dependent pressure gradient*, Indian J Pure Appl Math 8(9) (1977) 1124-1131.

[18] Ruchi Chaturvedi, R.K.Shrivatsav, Mohd. Salim Ahamad, *The numerical analysis of MHD flow of dusty visco-elastic first order oldroyd fluid when passing through a porous rectangular channel*, International Journal of Modern Mathematical Sciences, 9(1) (2014) 46-57.

[19] B.C.Prasannakumara, B.J.Gireesha, P.T.Manjunatha, *Melting phenomenon in MHD stagnation point flow of dusty fluid over a stretching sheet in the presence of thermal radiation and non-uniform heat source/sink*, International Journal for Computational Methods in Engineering Science and Mechanics , (2015) 1-18.

[20] Hai Long Liu, Junfeng Wang, Wook Ryol Hwang, *Flow resistance of viscoelastic flows in fibrous porous media*, Journal of Non-Newtonian Fluid Mechanics, 246 (2017) 21-30.

[21] Singh, C.B. Ram ,*Unsteady flow of a electrically conducting dusty viscous liquid through a channel*, Indian J. Pure and Appl. Math, 8(9)1977, 1022-1028.

[22] Prasad, V.R.Ramacharyulu, N.C.P, *Unsteady flow of a dusty fluid between two parallel plates under an impulsive pressure gradient*, Def. Sci, Journal, 38 (1979)125-130.

[23] Nag S.K, Jana R.N, Datta.N *Couette flow of a dusty gas* , Acta Mechanica, Springer Vertag, 3(1979)33, 179-187.

[24] C.S.Bagewadi and B.J.Gireesha, *A study of two dimensional unsteady fluid flow under varying pressure gradient,* Tensor, N.S. 64 (2003) 232-240.

[25] A.J.Chamka, *Unsteady laminar hydromagnetic fluid particle flow and heat transfer in channels and circular pipes*, Int. J. Heat and fluid flow, 21 (2000) 740-746.

[26] Parveen sharma and C.L.Varshney, *Thermal dispersion effect on MHD flow of dusty gas and dusty particles through hexagonal channel,* International journal of heat and mass transfer, 46 (2003) 2511-2514.

[27] P.T.Manjunatha, B.J.Gireesha, B.C.Prasannakumara, *Effect of Radiation on Flow and Heat Transfer of MHD Dusty Fluid Over a Stretching Cylinder Embedded in a Porous Medium in Presence of Heat Source*, Int J. Appl. Comput. Math (2015).

[28] Akhilesh K. Sahu, R.P.Chhabra, V. Eswaran, *Two dimensional unsteady laminar flow of a power law fluid across a square cylinder*, Journal of Non-Newtonian Fluid Mechanics, 160 (2009) 157-167.

[29] Michael Schriber, *Focus: The difference between round and square pipes*, Physical review letters, 8,94 (2015).

6. Appendix

$$c_1 = s + M + \epsilon_1 + \frac{a^2}{\eta(1-\phi)} + \frac{a^2r^2\pi^2}{d^2}, \quad c_2 = \epsilon_1, \ c_3 = \frac{\delta}{\phi'} - \frac{a^2r^2\pi^2}{d^2}, \ \ c_4 = \frac{s+\delta}{\phi'}, \ \lambda_1 = \frac{\beta a^2}{\nu},$$

$$c_{11} = \frac{\delta(d^2\left(M + \epsilon_1 + \frac{a^2}{\eta(1-\phi)}\right) + a^2r^2\pi^2) - \epsilon_1\left(\delta d^2 - a^2r^2\pi^2\phi'\right)}{d^2(\epsilon_1\phi' + \delta)}, \quad c_{12} = \epsilon_1\left(\delta d^2 - \phi' a^2r^2\pi^2\right),$$

$$c_{13} = d^2\left(M + \epsilon_1 + \frac{a^2}{\eta(1-\phi)}\right) + \delta d^2 + a^2r^2\pi^2, \ \ c_{14} = \delta d^2\left(M + \epsilon_1 + \frac{a^2}{\eta(1-\phi)}\right) + \delta a^2r^2\pi^2 - c_{12},$$

$$c_{15} = M + \epsilon_1 + \frac{a^2}{\eta(1-\phi)} + \frac{a^2r^2\pi^2}{d^2}, \ c_{16} = -d^2\lambda_1^2 + \delta d^2\left(M + \epsilon_1 + \frac{a^2}{\eta(1-\phi)}\right) + \delta a^2r^2\pi^2 - c_{12},$$

$$c_{17} = d^2\lambda_1\delta + d^2\left(M + \epsilon_1 + \frac{a^2}{\eta(1-\phi)}\right)\lambda_1 + a^2r^2\pi^2\lambda_1, \ c_{18} = M + \epsilon_1 + \frac{a^2}{\eta(1-\phi)} + \frac{a^2r^2\pi^2}{d^2} - \alpha_1,$$

$$A^2 = \frac{c_1c_4 - c_2c_3}{c_2 + c_4}, \ \alpha_1 = \frac{c_{16}\left(\epsilon_1\phi' + \delta\right) + \lambda_1 c_{17}}{d^2\left((\epsilon_1\phi' + \delta)^2\right) + \lambda_1^2}, \ \ \beta_1 = \frac{c_{17}\left(\epsilon_1\phi' + \delta\right) - \lambda_1 c_{16}}{d^2\left((\epsilon_1\phi' + \delta)^2\right) + \lambda_1^2}, \ \alpha_2 = \sqrt{\frac{\alpha_1 + \sqrt{\alpha_1^2 + \beta_1^2}}{2}},$$

$$\beta_2 = \sqrt{\frac{-\alpha_1 + \sqrt{\alpha_1^2 + \beta_1^2}}{2}}, \ y_1 = \frac{-b_{21} + \sqrt{b_{21}^2 - 4a_{21}c_{21}}}{2a_{21}}, \ \ y_2 = \frac{-b_{21} - \sqrt{b_{21}^2 - 4a_{21}c_{21}}}{2a_{21}},$$

$$a_{21} = 4d^2, \ \ b_{21} = 4d^2M + 4d^2\epsilon_1 + \frac{4d^2a^2}{\eta(1-\phi)} + 4\delta d^2 + 4a^2r^2\pi^2 + (2n+1)^2\pi^2d^2,$$

$$c_{21} = 4\delta d^2M + 4\delta d^2\epsilon_1 + \frac{4\delta d^2a^2}{\eta(1-\phi)} + 4\delta a^2r^2\pi^2 - 4\epsilon_1\delta d^2 + 4\epsilon_1\phi' a^2r^2\pi^2 + (2n+1)^2\pi^2d^2\epsilon_1\phi' + (2n+1)^2\pi^2d^2\delta,$$

$$C_1 = \frac{e^{y_1t}\left(\epsilon_1\phi' + y_1 + \delta\right)^2}{y_1\left[(\epsilon_1\phi' + y_1 + \delta)(2y_1d^2 + c_{13}) - (y_1^2d^2 + y_1c_{13} + c_{14})\right]}, E = \cosh(\alpha_2 y)\cos(\beta_2 y), \ \ G = \cosh(\alpha_2)\cos(\beta_2),$$

$$D_1 = \frac{e^{y_2t}\left(\epsilon_1\phi' + y_2 + \delta\right)^2}{y_2\left[(\epsilon_1\phi' + y_2 + \delta)(2y_2d^2 + c_{13}) - (y_2^2d^2 + y_2c_{13} + c_{14})\right]}, F = \sinh(\alpha_2 y)\sin(\beta_2 y), \ \ H = \sinh(\alpha_2)\sin(\beta_2)$$

$$C_2 = \frac{e^{y_1t}\left(y_1 + M + \epsilon_1 + \frac{a^2}{\eta(1-\phi)} + \frac{a^2r^2\pi^2}{d^2} + \frac{(2n+1)^2\pi^2}{4}\right)\left(\epsilon_1\phi' + y_1 + \delta\right)^2}{y_1\left[(\epsilon_1\phi' + y_1 + \delta)(2y_1d^2 + c_{13}) - (y_1^2d^2 + y_1c_{13} + c_{14})\right]},$$

$$D_2 = \frac{e^{y_2t}\left(y_2 + M + \epsilon_1 + \frac{a^2}{\eta(1-\phi)} + \frac{a^2r^2\pi^2}{d^2} + \frac{(2n+1)^2\pi^2}{4}\right)\left(\epsilon_1\phi' + y_2 + \delta\right)^2}{y_2\left[(\epsilon_1\phi' + y_2 + \delta)(2y_2d^2 + c_{13}) - (y_2^2d^2 + y_2c_{13} + c_{14})\right]},$$

$$C_3 = \frac{y_1e^{y_1t}\left(\epsilon_1\phi' + y_1 + \delta\right)^2}{(y_1^2 + \lambda_1^2)\left[(\epsilon_1\phi' + y_1 + \delta)(2y_1d^2 + c_{13}) - (y_1^2d^2 + y_1c_{13} + c_{14})\right]},$$

$$D_3 = \frac{y_2e^{y_2t}\left(\epsilon_1\phi' + y_2 + \delta\right)^2}{(y_2^2 + \lambda_1^2)\left[(\epsilon_1\phi' + y_2 + \delta)(2y_2d^2 + c_{13}) - (y_2^2d^2 + y_2c_{13} + c_{14})\right]}$$

$$X_1 = (EG + FH)\,c_{18} - (EH - FG)(\lambda_1 - \beta_1), \ \ X_2 = (EG + FH)(\lambda_1 - \beta_1) + c_{18}(EH - FG)$$

$$C_4 = \frac{y_1e^{y_1t}\left(y_1 + M + \epsilon_1 + \frac{a^2}{\eta(1-\phi)} + \frac{a^2r^2\pi^2}{d^2} + \frac{(2n+1)^2\pi^2}{4}\right)\left(\epsilon_1\phi' + y_1 + \delta\right)^2}{(y_1^2 + \lambda_1^2)\left[(\epsilon_1\phi' + y_1 + \delta)(2y_1d^2 + c_{13}) - (y_1^2d^2 + y_1c_{13} + c_{14})\right]},$$

$$D_4 = \frac{y_2e^{y_2t}\left(y_2 + M + \epsilon_1 + \frac{a^2}{\eta(1-\phi)} + \frac{a^2r^2\pi^2}{d^2} + \frac{(2n+1)^2\pi^2}{4}\right)\left(\epsilon_1\phi' + y_2 + \delta\right)^2}{(y_2^2 + \lambda_1^2)\left[(\epsilon_1\phi' + y_2 + \delta)(2y_2d^2 + c_{13}) - (y_2^2d^2 + y_2c_{13} + c_{14})\right]},$$